

Numerical study of the effect of orientation and infilling material of joint on the strength and deformation behavior of jointed rock

Majid Noorian-Bidgoli¹, Banafsheh Sadat Lajevardi¹

Received: 2025 Jan. 11, Revised: 2025 Feb. 27, Online Published: 2025 Mar. 01



Journal of Geomine © 2024 by University of Birjand is licensed under CC BY 4.0

ABSTRACT

This paper investigates the influence of two key properties of rock joints, namely orientation and infilling material, on the strength and deformation behavior of jointed rock. To achieve this objective, numerical experiments were conducted using the UDEC code based on the discrete element method (DEM). The simulations involved uniaxial compression tests on a limestone rock specimen with a single joint. Twelve models of jointed rock were created, incorporating three different types of infilling materials (F1, F2, and F3) and four joint orientation angles (0°, 45°, 60°, and 90°). A novel technique based on the equilibrium principle of the models during loading was employed to mimic realistic static loading conditions, ensuring controlled application of axial loads and preventing sudden catastrophic failure. Two-dimensional (2D) models were used to evaluate the computational models' uniaxial compressive strength (UCS) and stress-strain behavior. The results indicate that the combination of joint orientation angle and infilling material significantly influences jointed rock's strength and deformation behavior. Under pressure, the jointed rock models exhibit orientation and infilling material-dependent behaviors, leading to varying UCS values. The UCS of jointed rocks decreased as the orientation angles increased from 0 to 60 degrees, ranging from 25 MPa for the strongest infilling material (F1) at a joint orientation angle of 0° to 0.63 MPa for the weakest infilling material (F2) at a joint orientation angle of 60°. The maximum UCS values of jointed rock were observed at a joint orientation angle of 90°: 26.3 MPa for F1, 22.1 MPa for F2, and 24.1 MPa for F3 infilling materials. The deformation behaviors of the jointed rock are nonlinear and ductile, irrespective of the orientation and infilling materials of the rock joint. These findings highlight the importance of considering the combined effect of joint properties to reduce uncertainty in the strength and deformation parameters of jointed rock.

KEYWORDS

Uniaxial compressive strength (UCS), Deformation behavior, Numerical modeling, Discrete element method (DEM)

I. INTRODUCTION

Determining the properties of rock masses is a crucial aspect of geotechnical problems (Pine and Harrison, 2003). A rock mass consists of intact rock with discontinuities (Priest, 1993). However, determining their properties is challenging due to the complex and variable nature of rock masses (Zhang, 2016). The strength and deformability of rock masses are influenced by the inherent characteristics of intact rock and the presence of discontinuities within it (Noorian-Bidgoli, 2014). Consequently, rock masses cannot be treated as CHILE (continuous, homogeneous, isotropic, and linearly elastic) materials but rather as DIANE (discontinuous, inhomogeneous, anisotropic, and nonlinear elastic) materials (Hudson and Harrison, 2000). Strength is a critical parameter in rock mass engineering, as it significantly impacts rocks' mechanical behavior and fracture mechanisms (Qi et al., 2020). Given that most rock structures experience pressure, accurately determining the compressive strength of the rock mass

is of utmost importance (Gupta and Rao, 2000; Zhang, 2010), particularly for designing and analyzing the stability of various surface and subsurface structures.

Discontinuities encompass weak natural surfaces within the rock, including joints, faults, bedding planes, folds, schistosity planes, sheared zones, and faults (ISRM, 1978). With their diverse geometric and mechanical characteristics, discontinuities are pivotal in defining a rock mass (Wines and Lilly, 2003). Consequently, discontinuities within a rock mass lead to spatial heterogeneity and directional anisotropy (Noorian-Bidgoli and Jing, 2014). Moreover, each type of discontinuity possesses distinct characteristics that can influence the strength behavior of the rock mass (Han et al., 2022; Xu et al., 2024). For instance, joints, the most common type of discontinuity in nature, exhibit properties such as dip (Han et al., 2018), dip direction, or orientation (Kulatilake, 1985; Basu et al., 2009; Kumar et al., 2018), size or trace length (Cruden, 1977; Kulatilake, 1984), aperture (ISRM, 1978), frequency (Song, 2006), spacing (Priest and Hudson, 1976; Rives, 1992), infilling

¹ Department of Mining Engineering, Faculty of Engineering, University of Kashan, Kashan, Iran

✉ M. Noorian-Bidgoli: noriyan@kashanu.ac.ir

material (ISRM, 1978; Gong et al., 2018; Cui and Gratchev, 2020; Zhao et al., 2020), density (Jia et al., 2025), roughness (Shan et al., 2025), and persistence (Einstein et al., 1983; Kim et al., 2007; Das and Singh, 2020). These characteristics necessitate a comprehensive investigation when determining the strength behavior of the rock mass (Wu et al., 2022; Wang et al., 2025).

The uniaxial or unconfined compressive strength (UCS) serves as a widely employed metric for measuring rock strength (Hoek, 1983; Brook, 1993; Hoek and Brown, 1997; Wang et al., 2022). Various direct and indirect methods, including experimental, empirical, and theoretical-analytical approaches, can be employed to determine this strength (Hoek, 1977; Jade and Sitharam, 2003; Del Potro and Hürlimann, 2009; Que et al., 2021; Que et al., 2023; Li et al., 2025). Accurately estimating this property is essential for conducting any type of analysis in rock engineering design (Hoek, 2000).

Experimental methods encompass both in-situ (Bieniawski, 1968; Bieniawski and Van Heerden, 1975) and laboratory tests (Franklin and Chandra, 1972; Ramna and Venkatanarayana, 1973; Szlavín, 1974; Lama and Vutukuri, 1978; Reik and Zacas, 1978; Gaviglio, 1989; Gupta and Seshagiri, 1998; Al-Harhi, 1999; Starzec, 1999; Plinninger et al., 2003; Dinçer et al., 2004; Yaşar and Erdoğan, 2004; Aydın and Basu, 2005; Alber et al., 2007; Buyuksagis and Goktan, 2007; Ji et al., 2007; Kahraman and Yeken, 2008; Basu and Kamran, 2010; Kayabali and Selcuk, 2010; Rahmouni et al., 2013; Aydan et al., 2014; Aladejare, 2020; Zhong et al., 2020; Kumar et al., 2022; Singh and Khalkho, 2023; Zhao et al., 2025) that provide direct measurements of rock strength and deformation parameters (Özsan and Akin, 2002). Laboratory testing offers the advantage of assessing the compressive strength of small rock samples using precise and efficient measuring devices, following standardized protocols (Ulusay and Hudson, 2007). However, determining the UCS of the entire rock mass in the laboratory is challenging since it requires intact and large samples that accurately represent the conditions of discontinuities within the rock. Consequently, the results obtained from small rock samples may not reflect reality. To address this limitation, in-situ field tests employing various devices (Fig. 1) have been developed to directly assess the strength and deformation parameters of rock masses (Rix et al., 2019). While these methods yield results closer to reality, they are often time-consuming, costly, and associated with implementation difficulties.

Given the drawbacks and complexities of direct methods, several empirical approaches (Karakul and Ulusay, 2013) have been developed to estimate rock

strength indirectly. Some of these methods fall under the category of rock mass classification systems, drawing on experiences gained from diverse engineering projects (Hashemi et al., 2010; Singh and Goel, 2011). Notable empirical methods include rock mass rating (RMR) (Bieniawski, 1974), geological strength index (GSI) (Sonmez and Ulusay, 1999; Cai et al., 2004; Huang et al., 2019), and rock mass index (RMi) (Palmström, 1996). Failure criteria, such as the Hoek–Brown criterion (Hoek et al., 2002), can also be used to predict the strength parameters of rock masses (Bagheripour et al., 2011). One advantage of these methods is their simplicity, as they do not require numerous parameters to estimate rock mass strength. However, their results tend to be less accurate and reliable due to the omission of influential factors, such as the characteristics of discontinuities. Additionally, since the development of these methods is based on data obtained from specific regions, their applicability may be limited in other locations.

Given the limitations and drawbacks of practical and empirical methods in estimating rock mass strength, it is crucial to develop a precise and essential method that can effectively assess the impact of discontinuities on rock mass strength. Theoretical-analytical methods fall under indirect approaches, capable of simulating real-world problems using mathematical frameworks (Lawal et al., 2022). These methods can be classified into two categories: novel and numerical methods.

Novel methods encompass computational analytical techniques that employ mathematical modeling to determine optimal values in complex problems, considering various objectives and constraints. These methods often draw on operations research techniques such as linear and nonlinear programming, Monte-Carlo simulation, and others (Grima and Babuška, 1999; Meulenkamp and Grima, 1999; Gokceoglu, 2002; Gokceoglu and Zorlu, 2004; Tiryaki, 2008; Zorlu et al., 2008; Beiki et al., 2010; Dehghan et al., 2010; Cevik et al., 2011; Mishra and Basu, 2013; Wang and Aladejare, 2015; Jahed Armaghani et al., 2018; Aliyu et al., 2019; Gupta and Natarajan, 202; Dadhich et al., 2022; Zhang et al., 2022). Artificial neural networks (ANN), neural-fuzzy inference systems (ANFIS), and evolutionary, machine learning techniques and meta-heuristic algorithms (Fattahi and Hasanipanah, 2021; Jing et al., 2021; Lei et al., 2022; Li et al., 2023; Li et al., 2023; Yu et al., 2023), among others, can also be utilized in this context. While these methods offer high flexibility, reduced computational time, and the ability to consider quantitative and qualitative criteria, their reliance on random processes can lead to irreproducible results, introducing uncertainty and unreliability.

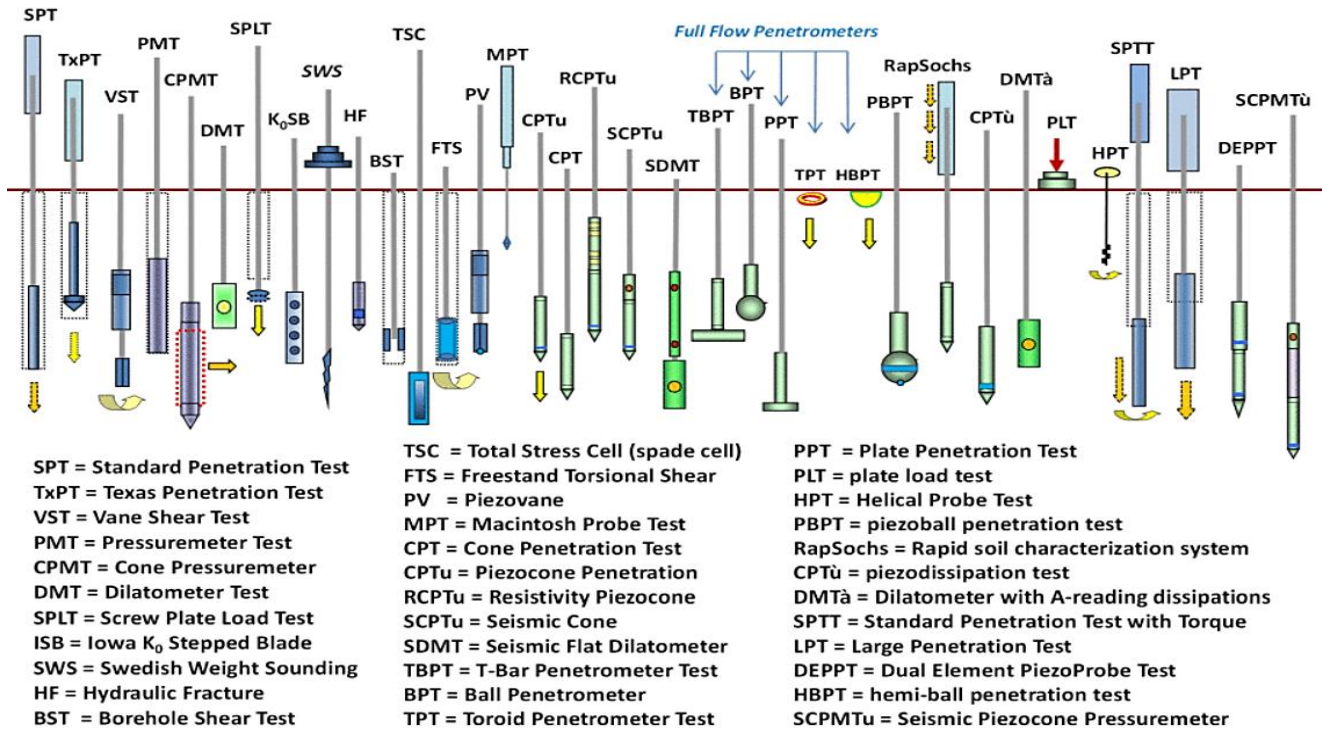


Fig. 1. The in-situ field tests for rock mass characterization (Rix et al., 2019)

On the other hand, numerical methods provide highly accurate calculations based on differential or integral equations, solving complex problems that may be challenging or impossible to solve with other techniques (Jing and Hudson, 2002; Tang et al., 2020). Previous research has demonstrated the reliability of numerical methods in modeling rock masses (Tang et al., 2000; Kulatilake et al., 2001; Min and Jing, 2003; Xu et al., 2013; Seshagiri Rao, 2020; Li and Zhao, 2021). In most numerical methods, the behavior of the rock mass is assessed by dividing it into numerous small elements and analyzing their behavior (Kulatilake et al., 2015; Guo et al., 2016). The fundamental requirement for the numerical analysis is dividing the rock mass into elements with similar properties and characteristics based on geological studies and rock engineering classifications. An outstanding feature of this method is the creation of continuous or discontinuous models comprising structural complexities and rock blocks, enabling more accurate analysis. The choice between continuous and discontinuous models depends on various factors specific to the problem, such as scale, joint system geometry, and discontinuities and spacing.

The Discrete Element Method (DEM) is a numerical method widely used in rock mechanics for analyzing discontinuous media (Jing, and Stephansson, 2007; Shimizu et al., 2010). Initially introduced by Cundall in 1974, DEM focuses on investigating the deformation of rock blocks by treating discontinuities as boundaries between these blocks (Cundall, 1980; Cundall and Hart, 1992). Rather than individual block failure, DEM considers failure as the movement of blocks along

discontinuities (Choi and Coulthard, 2020). This approach is particularly suitable when the displacement of discontinuities dominates over block deformation. Due to its high accuracy, DEM has become a prevalent method for stress-deformation analysis in various fractured rock structures (Alshkane et al., 2017).

The Universal Distinct Element Code (UDEC) is a powerful two-dimensional numerical program based on the discrete element method (DEM), capable of modeling fractured rock masses with rock blocks and fractures (Itasca, 2004; Lawankar et al., 2024; Jaber and Zare, 2025; Zhang et al., 2025). The model represents a collection of discrete blocks separated by joints, allowing the investigation of stress-strain behavior by selecting a constitutive model for the rock mass.

To obtain realistic results regarding the properties of rock masses, it is essential to conduct tests on rock samples containing discontinuities. In practical engineering applications, rock structures contain many joints with infilling material in varying orientations. The strength and deformation behavior of jointed rock filled with material is unclear. Therefore, it is necessary to investigate the mechanical behavior of filled jointed rocks under compression conditions.

In this study, we investigate the influence of joints, a common type of discontinuity in rock masses, on the strength and deformability of the rock. Specifically, we focus on two critical characteristics of joints: orientation and infilling material, and their impact on the uniaxial compressive strength of the rock. To achieve this, we employ the discrete element numerical method (DEM) using the UDEC code to simulate uniaxial compression

tests on a limestone sample containing a single joint. Subsequently, we conduct a sensitivity analysis to explore how joint parameters affect the strength and deformability of the rock model.

II. NUMERICAL MODELING PROCEDURE

In this study, we simulate uniaxial compressive strength tests on a jointed rock model using UDEC code. Numerical prediction through discrete element methods (DEM) is an effective approach for modeling. DEMs provide explicit representations of joint system geometry and their constitutive behaviors, as well as those of intact rock. To achieve this, an investigation was conducted using numerical experiments simulating typical laboratory compression tests to determine jointed rock models' compressive strength and deformation parameters. Fig. 2 illustrates the flowchart utilized in this study for a numerical strength-deformation analysis process in jointed rock using UDEC. The uniaxial compressive loading conditions are consistent with standard laboratory tests for intact rock samples.

To begin, we create a model geometry that resembles a cylindrical rock sample typically used in laboratory testing. The two-dimensional model takes the form of a rectangular shape with dimensions of 0.109 meters in length and 0.054 meters in width. Each model consists of an intact rock specimen with a single joint positioned at the center, varying in orientation and infilling materials.

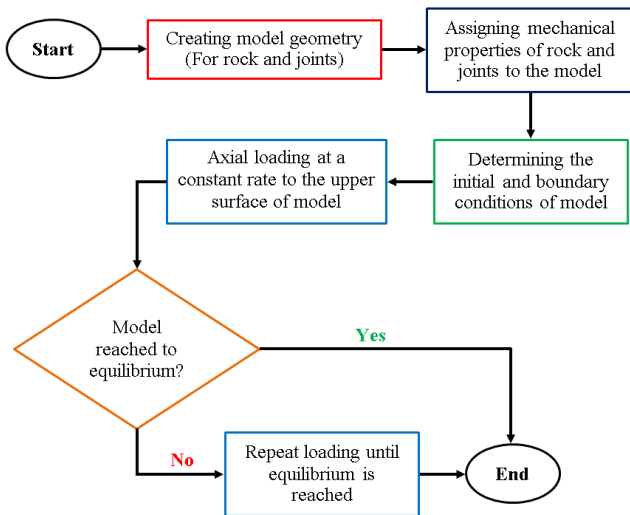


Fig. 2. Flowchart for a numerical strength-deformation analysis process in a jointed rock using UDEC

To examine the influence of joint orientation on uniaxial compressive strength, we utilize four models with orientation angles of 0°, 45°, 60°, and 90°. Additionally, to explore the impact of joint infilling material, we employ three types of infilling materials (F1, F2, and F3) with distinct mechanical properties (Table 1) for each model. Thus, 12 models (four joint

orientation angles combined with three infilling material types) are developed for this research.

Table 1. Material properties of joint infilling material

Property	Infilling material type		
	F1	F2	F3
Uniaxial compressive strength (MPa)	3.92	0.62	2.20
Friction angle (°)	32.10	34.34	36.34
Cohesion (MPa)	0.106	0.278	0.17

The mechanical properties of the intact rock in our study are similar to those used by Mokhtarian et al (2020) for a specific limestone type. The relevant mechanical properties of limestone and the joint are provided in Table 2. We adopt the Mohr-Coulomb behavior model to assign material properties to the jointed rock model, as the necessary parameters are readily available.

Table 2. Material properties of intact rock and joint

Mechanical properties		Value
Intact rock	Density	2700 Kg/m ³
	Young's modulus	96 GPa
	Poisson's ratio	0.37
	Friction angle	25.67°
	Cohesion	9.17 MPa
Joint	Joint normal stiffness (K _n)	1000 GPa/m
	Joint shear stiffness (K _s)	1000 GPa/m

Upon assigning the mechanical properties to the jointed rock model, the software automatically generates the mesh for the model. The meshing process for the four orientation angles is illustrated in Fig. 3.

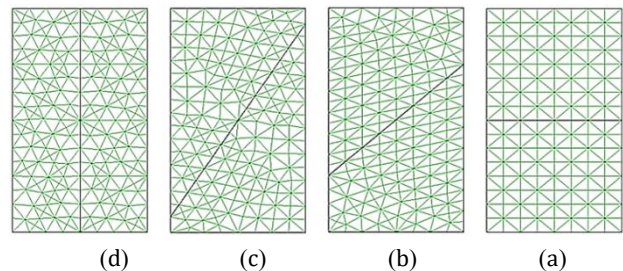


Fig. 3. Geometry and meshing of the jointed rock model with joint's orientation of (a) 0°, (b) 30°, (c) 45°, and (d) 90°

Next, we proceed to simulate the uniaxial compression test by applying a uniform and continuous load (y) to the upper surface of the model (Fig. 4). The calculation involves adding the increment in vertical forces (Δy) to the sum of forces applied from previous time steps ($y + \Delta y$). Typically, a lower loading rate requires more time but yields higher calculation accuracy. In this research, we assume an axial loading rate of 0.05 MPa per second.

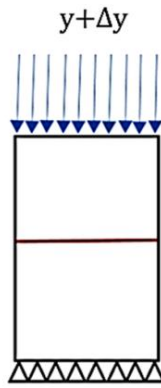


Fig. 4. Boundary conditions of the model in uniaxial compressive strength test

Before running the model with applied boundary conditions, efforts are made to replicate laboratory conditions for loading. As depicted in Fig. 4, the displacement at the lower level of the model is assumed to be zero in both the x and y directions. By fixing the displacement of the two side walls of the model along the y-axis, we allow movement of these boundaries only along the x-axis.

Observation points on the model are commonly utilized to monitor and analyze changes in displacement, stress, strain, etc., during the simulation stages. For this research, we employ nine observation points. These points consist of four corner points (two upper and two lower); one at the center of the upper surface, one at the center of the lower surface, one at the model's center, and two at the beginning and end of the joint. Among these points, the location of the two points on the model joint differs depending on the joint's orientation. Fig. 5 illustrates the defined locations for recording observation points in each model. These points serve to verify the model's equilibrium during loading.

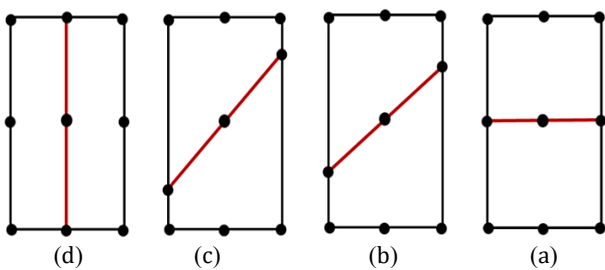


Fig. 5. Schematic of the location of 9 observation points on the jointed rock model with joint's orientation of (a) 0°, (b) 30°, (c) 45°, and (d) 90°

The discrete element method relies on explicit solutions, making the time step crucial in each model run. When the automatic mode is selected during model execution, the overall equilibrium of the model is typically the criterion for determining the end of problem-solving. In this research, an innovative method has been employed to ensure that every point in the model reaches equilibrium at each implementation step. This method has been previously used and validated in

the author's earlier research (Noorian-Bidgoli et al., 2013). While this method is more time-consuming than conventional approaches involving loop definition, it yields accurate results.

Typically, in numerical modeling with loop definition, the model is automatically saved, and the next step is executed after each run. However, the method used in this research follows a different approach. After each loading during a specific cycle and model run, the history of unbalanced forces is examined at all observation points. If the unbalanced forces have reached zero or are close to zero over time, the model is manually saved, and the next cycle begins. If the model has not yet reached equilibrium, it requires further cycles. This execution process is repeated systematically until the rock model reaches its ultimate strength. Fig. 6 illustrates the complete history of unbalanced forces for the first ten steps in the single-joint model with a 45° orientation angle and infilling material type F1.

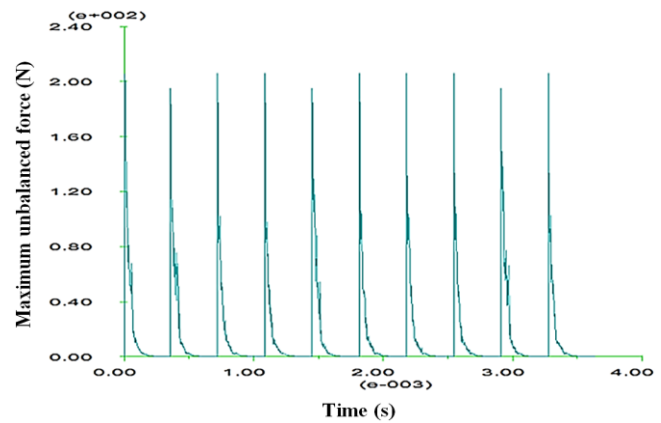


Fig. 6. Variations of unbalanced forces concerning time during the uniaxial compressive strength test

Table 3 presents the number of steps performed in each model. It is evident that the number of model execution steps increases as the joint's orientation angle increases. Furthermore, the model with infilling material type F2 requires more execution steps compared to other models.

TABLE 3. NUMBER OF EXECUTED STEPS IN EACH JOINTED MODEL

Joint's orientation (°)	Infilling material type		
	F1	F2	F3
0	6258300	6993000	6119700
45	11002300	11554750	7885070
60	12225550	12998250	10078300
90	13227160	13259970	12888450

In the DEM, due to the physical presence of damping in nature and the depreciation of energy, as well as the numerical stability of calculations, damping should be used somehow to minimize the kinetic energy of this dynamic system. Therefore, in this modeling, local damping has been used to minimize the fluctuations caused by model failure.

The uniaxial compressive strength (UCS) obtained from modeling was compared to the UCS measured during experimental tests (Mokhtarian et al., 2020) to validate the numerical models. This comparison was conducted for jointed rock samples with infilling material type F1 and joint orientation angles of 0°, 45°, 60°, and 90° (Fig. 7). This process quantitatively measures how closely the model's predictions agree with experimental observations. However, this figure clearly shows that the results agree with each other. The UCS values confirm that the simulation process was conducted correctly.

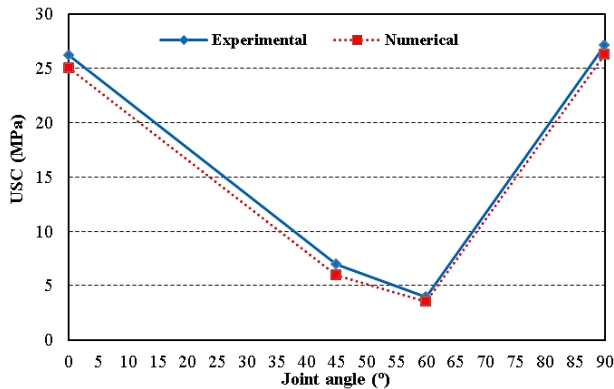


Fig. 7. Comparison of experimental and numerical UCS values for rock samples containing infilling material type F1 and with joint orientation angles of 0°, 45°, 60°, and 90°

III. RESULTS AND DISCUSSION

In the DEM, the application of an external force to the surface unit (stress) creates irregularities that are propagated through successive contacts between the blocks. Each rock block is influenced by force exerted by its adjacent block, following Newton's second law, resulting in strain within the model. This research focuses on obtaining axial stress-axial strain curves after each model implementation.

Fig. 8 displays the stress-strain curve for the case where the joint orientation angle is zero degrees. The graph reveals that the uniaxial compressive strength of the model remains similar across the three types of joint infilling material. This suggests that when the loading direction is perpendicular to the joint orientation, the type of infilling material has minimal impact on the uniaxial compressive strength of the jointed rock model.

Furthermore, Fig. 9 presents the stress-strain curve for a joint orientation angle of 45 degrees. In this case, models with infilling materials F1 and F3 exhibit the lowest and highest uniaxial compressive strength, respectively. Referring to Table 1, which lists the mechanical properties of the infilling materials, it is evident that the uniaxial compressive strength of the jointed rock model is proportional to the friction angles of the infilling material. Specifically, infilling materials F1 and F3 possess the lowest and highest friction angles, respectively. Consequently, it can be concluded that the friction angles of the infilling material play a significant

role in determining the uniaxial compressive strength of the jointed rock model at this orientation angle.

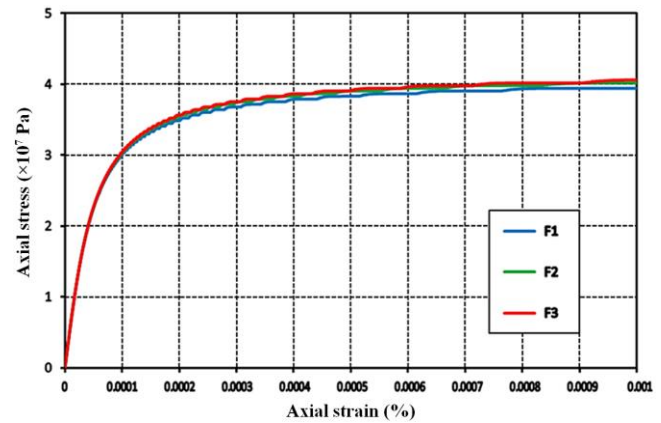


Fig. 8. Axial stress versus axial strain curves for jointed rock model with varying infilling materials and joint orientation angle equal to zero degrees

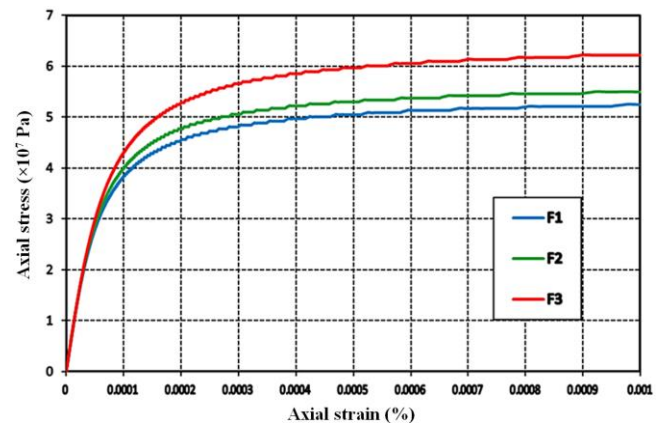


Fig. 9. Axial stress versus axial strain curves for jointed rock model with varying infilling materials and joint orientation angle equal to 45 degrees

Similarly, Fig. 10 illustrates the stress-strain curve for a joint orientation angle of 60 degrees. In this scenario, models with infilling materials F1 and F2 exhibit the lowest and highest uniaxial compressive strength, respectively. Again, referring to Table 1, the uniaxial compressive strength of the jointed rock model is proportional to the cohesion of the infilling material. Notably, infilling materials F1 and F2 possess the lowest and highest cohesion, respectively. Thus, it can be concluded that the cohesion of the infilling material significantly influences the uniaxial compressive strength of the jointed rock model at this orientation angle.

Fig. 11 presents the stress-strain curve for the case where the joint orientation angle is 90 degrees. As depicted in the graph, models with infilling materials F3 and F1 exhibit the lowest and highest uniaxial compressive strength, respectively. Referring to Table 1, which lists the mechanical properties of the infilling materials, it becomes evident that the uniaxial compressive strength of the jointed rock model is proportional to the uniaxial compressive strength of the

joint infilling material. Notably, infilling material F1 possesses the highest uniaxial compressive strength. Therefore, it can be concluded that, at this orientation angle, the uniaxial compressive strength of the joint infilling material significantly affects the uniaxial compressive strength of the jointed rock model.

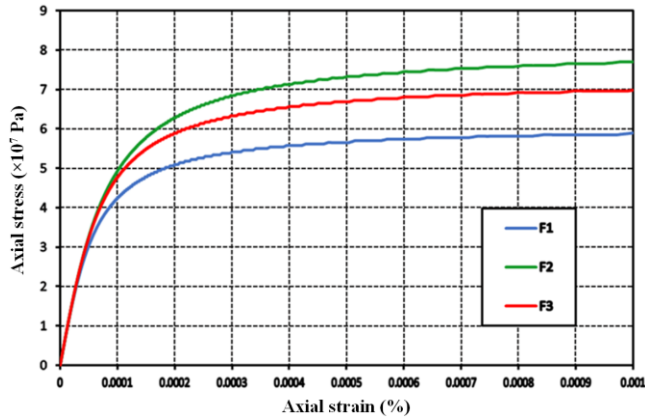


Fig. 10. Axial stress versus axial strain curves for jointed rock model with varying infilling materials and joint orientation angle equal to 60 degrees

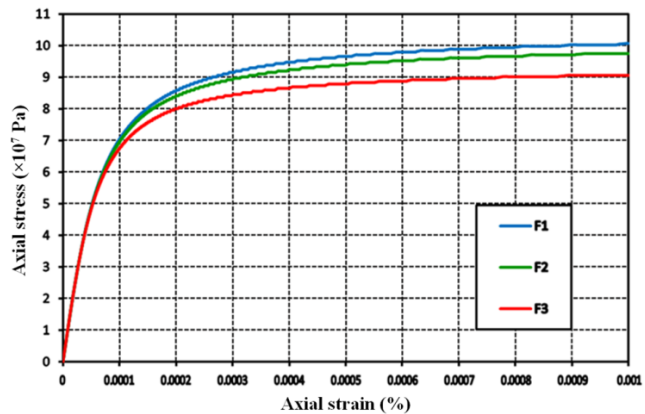


Fig. 11. Axial stress versus axial strain curves for jointed rock model with varying infilling materials and joint orientation angle equal to 90 degrees

Furthermore, comparing these results with those obtained for a joint orientation angle of 45 degrees (Fig. 9) reveals a reversal of outcomes due to a 45-degree increase in joint orientation in the counterclockwise direction. This emphasizes the importance of considering anisotropy when determining the compressive strength of jointed rock. The findings indicate that anisotropy can more substantially impact the compressive strength of jointed rock than the type of joint-infilling material.

Fig. 12 compares the stress-strain curves for all 12 models investigated in this research. A significant finding from this figure is that irrespective of the joint orientation, the deformation behavior of all the studied models exhibits nonlinear ductile characteristics. This suggests that the presence of discontinuities can transform the deformation behavior of jointed rock from brittle to ductile. Moreover, in addition to the mechanical

properties of the joint's infilling materials, anisotropy plays a crucial role in estimating the uniaxial compressive strength of the jointed rock. As the loading direction aligns more closely with the joint orientation, the uniaxial compressive strength of the model increases. Specifically, the highest uniaxial compressive strengths of the jointed model are observed when the loading direction is perpendicular and parallel to the joint orientation, respectively. Notably, as the joint orientation increases counterclockwise from 0° to 90°, the yield point representing the model's transition from elastic to plastic behavior also increases. This suggests a direct relationship between the uniaxial compressive strength and the yield point of the model. Higher yield strength corresponds to higher uniaxial compressive strength. Furthermore, comparing the results reveals that an increase in joint orientation counterclockwise (from 0° to 90°) leads to an increase in Young's modulus, which is reflected in the slope of the stress-strain curve in the elastic region.

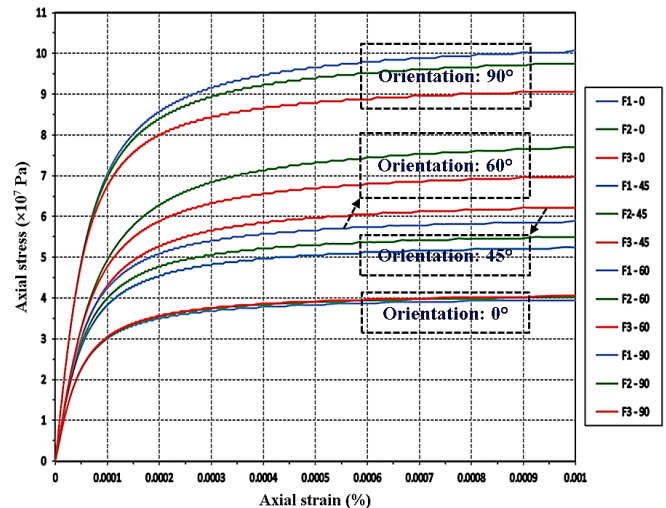


Fig. 12. Axial stress versus axial strain curves for jointed rock model with varying infilling materials and joint orientation angles

Table 4 shows the uniaxial compressive strength (UCS) obtained from modeling jointed rock samples that contain three types of infilling materials (F1, F2, and F3) at joint orientation angles of 0°, 45°, 60°, and 90°. As shown in this table, the composition of infill materials significantly impacts the unconfined compressive strength (UCS) along the joint's orientation. The uniaxial compressive strength of jointed rock models depends on the strength of the filler material. The jointed rock models that use infill materials with higher strength (F1) exhibit a greater UCS at all joint orientation angles. The UCS decreased as the orientation angles increased from 0 to 60 degrees, with the minimum axial strength occurring at 60 degrees. The maximum UCS values of jointed rock models were obtained at joint orientation angles 90° for all infilling materials.

Table 4. the uniaxial compressive strength values (MPa) of jointed rock models

Joint's orientation (°)	Infilling material type		
	F1	F2	F3
0	25	21.6	15.9
45	6	1.19	3.9
60	3.5	0.68	3
90	26.3	22.1	24.1

The results indicate that the combination of infill materials and orientation angles significantly influences the UCS of jointed rock. These findings emphasize the need to consider the combined effects of joint properties to minimize uncertainty in the strength and deformation parameters of jointed rock, which is very important in rock engineering applications.

IV. CONCLUSION

This study aimed to systematically investigate the influence of infilling materials and joint orientation on the compressive strength and deformation behavior of jointed rock. Utilizing the discrete element method (DEM), 2D numerical experiments were conducted on 12 geometric models of limestone rock samples with single joints. An innovative aspect of this research was implementing the unbalanced force monitoring technique, which allowed for simulating a quasi-static state of equilibrium similar to a standard servo-controlled test. The key findings of this study can be summarized as follows:

1. The joint orientation significantly impacts the strength and deformation behavior of jointed rock. The uniaxial compressive strength decreased as the orientation angles increased from 0 to 60 degrees, with the minimum axial strength occurring at 60 degrees. The maximum UCS values of jointed rock models were obtained at joint orientation angles 90° for all infilling materials. Therefore, anisotropy plays a crucial role in determining the strength and deformability of jointed rock, highlighting the importance of considering this factor in practical applications.

2. Analysis of the stress-strain curves revealed that the uniaxial compressive strength (UCS), Young's modulus, and yield strength of the jointed rock vary considerably with the joint's orientation.

3. When the axial loading direction aligns more closely with the joint orientation, the uniaxial compressive strength increases. The highest UCS values for jointed rock occur at a joint orientation angles 90° for all infilling materials. Therefore, the maximum UCS of the jointed model was observed when the axial loading direction was parallel to the joint orientation.

4. The type of infilling material plays a significant role in determining the uniaxial compressive strength (UCS) of jointed rock. The strength of the filler material directly affects the UCS of jointed rock models. Models that utilize infill materials with higher strength (F1) demonstrate greater UCS across all joint orientation angles.

5. The friction angle, cohesion, and UCS of the joint's infilling materials were influential factors in determining the uniaxial compressive strength of the jointed rock at different joint orientations. Hence, the mechanical properties of the joint's infilling materials significantly affect the uniaxial compressive strength of the jointed rock.

6. The deformation behavior of the jointed rock was consistently nonlinear and ductile, regardless of the joint orientation and infilling materials.

In further research, the authors plan to expand their investigation to include the effects of discontinuity characteristics on the strength and deformation behavior of rock with multiple joints. However, it is essential to incorporate additional infill materials and test them under various loading conditions to gain a more comprehensive understanding of the strength and deformation behavior of jointed rock masses. Moreover, the joint surface's roughness should be considered, as it significantly affects strength and deformation behavior. Future research could focus on these factors by examining the impacts of surface roughness and different compositions of infill materials. This approach would enhance our understanding of how jointed rocks behave in real-world conditions.

REFERENCES

- Aladejare, A. E. (2020). Evaluation of empirical estimation of uniaxial compressive strength of rock using measurements from index and physical tests. *Journal of Rock Mechanics and Geotechnical Engineering*, 12(2), 256-268. <https://doi.org/10.1016/j.jrmge.2019.08.001>
- Alber, M., Yaralı, O., Dahl, F., Bruland, A., Käsling, H., Michalakopoulos, T. N., Cardu, M., Hagan, P., Aydın, H., and Özarslan, A. (2015). ISRM suggested method for determining the abrasivity of rock by the CERCHAR abrasivity test. *The ISRM suggested methods for rock characterization, testing and monitoring: 2007-2014*, 101-106. <https://doi.org/10.1007/s00603-013-0518-0>
- Al-Harhi, A. A., Al-Amri, R. M., and Shehata, W. M. (1999). The porosity and engineering properties of vesicular basalt in Saudi Arabia. *Engineering Geology*, 54(3-4), 313-320. [https://doi.org/10.1016/S0013-7952\(99\)00050-2](https://doi.org/10.1016/S0013-7952(99)00050-2)
- Aliyu, M. M., Shang, J., Murphy, W., Lawrence, J. A., Collier, R., Kong, F., and Zhao, Z. (2019). Assessing the uniaxial compressive strength of extremely hard cryptocrystalline flint. *International Journal of Rock Mechanics and Mining Sciences*, 113: 310-321. <https://doi.org/10.1016/j.ijrmms.2018.12.002>
- Alshkane, Y. M., Marshall, A. M., and Stace, L. R. (2017). Prediction of strength and deformability of an interlocked blocky rock mass using UDEC. *Rock Mechanics and Geotechnical Engineering*, 9(3), 531-542. <https://doi.org/10.1016/j.jrmge.2017.01.002>
- Aydan, Ö., Sato, A., and Yagi, M. (2014). The inference of geo-mechanical properties of soft rocks and their degradation from needle penetration tests. *Rock mechanics and rock engineering*, 47, 1867-1890. <https://doi.org/10.1007/s00603-013-0477-5>
- Aydın, A., and Basu, A. (2005). The Schmidt hammer in rock material characterization. *Engineering Geology*, 81(1), 1-14. <https://doi.org/10.1016/j.enggeo.2005.06.006>
- Bagheripour, M. H., Rahgozar, R., Pashnesaz, H., and Malekinejad, M. (2011). A complement to Hoek-Brown failure criterion for strength prediction in anisotropic rock. *Geomechanics and Engineering*, 3(1), 61-81. <https://doi.org/10.12989/gae.2011.3.1.061>
- Basu, A., and Kamran, M. (2010). Point load test on schistose rocks and its applicability in predicting uniaxial compressive strength. *International journal of rock mechanics and mining sciences*, 47(5), 823-828. <https://doi.org/10.1016/j.ijrmms.2010.04.006>

- Basu, A., Celestino, T. B., Bortolucci, A. A. (2009). Evaluation of rock mechanical behaviors under uniaxial compression with reference to assessed weathering grades. *Rock Mechanics and Rock Engineering*, 42, 73-93. <https://doi.org/10.1007/s00603-008-0170-2>
- Beiki, M., Bashari, A., and Majidi, A. (2010). Genetic programming approach for estimating the deformation modulus of rock mass using sensitivity analysis by neural network. *International journal of rock mechanics and mining sciences*, 47(7), 1091-1103. <https://doi.org/10.1016/j.ijrmm.2010.07.007>
- Bieniawski, Z.T. (1968). In situ strength and deformation characteristics of coal. *Engineering Geology*, 2(5), 325-340. [https://doi.org/10.1016/0013-7952\(68\)90011-2](https://doi.org/10.1016/0013-7952(68)90011-2)
- Bieniawski, Z. T. (1974). Estimating the strength of rock materials. *Journal of the Southern African Institute of Mining and Metallurgy*, 74(8), 312-320. https://hdl.handle.net/10520/AJA0038223X_382
- Bieniawski, Z. T., Van Heerden, W. L. (1975). The significance of in situ tests on large rock specimens. *International Journal of Rock Mechanics and Mining Sciences & Geomechanics Abstracts*, 12(4), 101-113. [https://doi.org/10.1016/0148-9062\(75\)90004-2](https://doi.org/10.1016/0148-9062(75)90004-2)
- Brook, N. (1993). The measurement and estimation of basic rock strength. *Rock testing and site characterization*, 41-66. <https://doi.org/10.1016/B978-0-08-042066-0.50009-4>
- Buyuksagis, I. S., Goktan, R. (2007). The effect of Schmidt hammer type on uniaxial compressive strength prediction of rock. *International Journal of Rock Mechanics and Mining Sciences*, 44(2), 299-307. <https://doi.org/10.1016/j.ijrmm.2006.07.008>
- Cai, M., Kaiser, P. K., Uno, H., Tasaka, Y., Minami, M. (2004). Estimation of rock mass deformation modulus and strength of jointed hard rock masses using the GSI system. *International Journal of Rock Mechanics and Mining Sciences*, 41(1), 3-19. [https://doi.org/10.1016/S1365-1609\(03\)00025-X](https://doi.org/10.1016/S1365-1609(03)00025-X)
- Cevik, A., Sezer, E. A., Cabalar, A. F., Gokceoglu, C. (2011). Modeling of the uniaxial compressive strength of some clay-bearing rocks using neural network. *Applied Soft Computing*, 11(2), 2587-2594. <https://doi.org/10.1016/j.asoc.2010.10.008>
- Choi, S. K., Coulthard, M. A. (2020). Modelling of jointed rock masses using the distinct element method. *Mechanics of jointed and faulted rock*, 471-477. <https://doi.org/10.1201/9781003078975-66>
- Cruden, D.M. (1977). Describing the size of discontinuities. *International Journal of Rock Mechanics and Mining Sciences & Geomechanics Abstracts*, 14(3), 133-137. [https://doi.org/10.1016/0148-9062\(77\)90004-3](https://doi.org/10.1016/0148-9062(77)90004-3)
- Cui, C., Gratchev, I. (2020). Effects of pre-existing cracks and infillings on strength of natural rocks—cases of sandstone, argillite and basalt. *Journal of Rock Mechanics and Geotechnical Engineering*, 12(6), 1333-1338. <https://doi.org/10.1016/j.jrmge.2020.03.008>
- Cundall, P. A. (1980). UDEC-A Generalised Distinct Element Program for Modelling Jointed Rock. Cundall (Peter) Associates Virginia Water (England)
- Cundall, P. A., Hart, R. D. (1992). Numerical modelling of discontinua. *Engineering computations*, 9(2), 101-113. <https://doi.org/10.1108/eb023851>
- Dadhich, S., Sharma, J. K., Madhira, M. (2022). Prediction of Uniaxial Compressive Strength of Rock Using Machine Learning. *Journal of The Institution of Engineers (India): Series A*, 103(4), 1209-1224. <https://doi.org/10.1007/s40030-022-00688-4>
- Das, R., Singh, T. N. (2021). Effect of closely spaced, non-persistent ubiquitous joint on tunnel boundary deformation: a case study from Himachal Himalaya. *Geotechnical and Geological Engineering*, 39, 2447-2459. <https://doi.org/10.1007/s10706-020-01600-2>
- Dehghan, S., Sattari, G. H., Chelgani, S. C., Aliabadi, M. A. (2010). Prediction of uniaxial compressive strength and modulus of elasticity for Travertine samples using regression and artificial neural networks. *Mining Science and Technology*, 20(1), 41-46. [https://doi.org/10.1016/S1674-5264\(09\)60158-7](https://doi.org/10.1016/S1674-5264(09)60158-7)
- Del Potro, R., Hürliemann, M. (2009). A comparison of different indirect techniques to evaluate volcanic intact rock strength. *Rock Mechanics and Rock Engineering*, 42, 931-938. <https://doi.org/10.1007/s00603-008-0001-5>
- Diñcer, I., Acar, A., Çobanoğlu, I., Uras, Y. (2004). Correlation between Schmidt hardness, uniaxial compressive strength and Young's modulus for andesites, basalts and tuffs. *Bulletin of Engineering Geology and the Environment*, 63, 141-148. <https://doi.org/10.1007/s10064-004-0230-0>
- Einstein, H. H., Veneziano, D., Baecher, G. B., O'reilly, K. J. (1983). The effect of discontinuity persistence on rock slope stability. *International journal of rock mechanics and mining sciences & geomechanics abstracts*, 20(5), 227-236. [https://doi.org/10.1016/0148-9062\(83\)90003-7](https://doi.org/10.1016/0148-9062(83)90003-7)
- Fattahi, H., Hasanipanah, M. (2021). Predicting the shear strength parameters of rock: a comprehensive intelligent approach. *Geomechanics and Engineering*, 27(5), 511-525. DOI: <https://doi.org/10.12989/gae.2021.27.5.511>
- Franklin, J. A., Chandra, R. (1972). The slake-durability test. *International Journal of Rock Mechanics and Mining Sciences & Geomechanics Abstracts*, 9(3), 325-328. [https://doi.org/10.1016/0148-9062\(72\)90001-0](https://doi.org/10.1016/0148-9062(72)90001-0)
- Gaviglio, P. (1989). Longitudinal waves propagation in a limestone: the relationship between velocity and density. *Rock Mechanics and Rock Engineering*, 22(4), 299-306. <https://doi.org/10.1007/BF01262285>
- Gokceoglu, C. (2002). A fuzzy triangular chart to predict the uniaxial compressive strength of the Ankara agglomerates from their petrographic composition. *Engineering Geology*, 66(1-2), 39-51. [https://doi.org/10.1016/S0013-7952\(02\)00023-6](https://doi.org/10.1016/S0013-7952(02)00023-6)
- Gokceoglu, C., Zorlu, K. (2004). A fuzzy model to predict the uniaxial compressive strength and the modulus of elasticity of a problematic rock. *Engineering Applications of Artificial Intelligence*, 17(1), 61-72. <https://doi.org/10.1016/j.engappai.2003.11.006>
- Gong, L., Nemcik, J., Ren, T. (2018). Numerical simulation of the shear behavior of rock joints filled with unsaturated soil. *International Journal of Geomechanics*, 18(9), p.04018112. [https://doi.org/10.1061/\(ASCE\)GM.1943-5622.000125](https://doi.org/10.1061/(ASCE)GM.1943-5622.000125)
- Grima, M. A., Babuška, R. (1999). Fuzzy model for the prediction of unconfined compressive strength of rock samples. *International journal of rock mechanics and mining sciences*, 36(3), 339-349. [https://doi.org/10.1016/S0148-9062\(99\)00007-8](https://doi.org/10.1016/S0148-9062(99)00007-8)
- Guo, S., Qi, S., Li, X., Zou, Y., Zhang, S. (2016). Strength and deformation characteristics of rock sample with discontinuities under numerical uniaxial compression simulation tests. *Journal of Engineering Geology*, 24(5), 891-898. <https://doi.org/10.1016/j.jrmge.2020.03.008>
- Gupta, A. S., Rao, K. S. (2000). Weathering effects on the strength and deformational behaviour of crystalline rocks under uniaxial compression state. *Engineering geology*, 56(3-4), 257-274. [https://doi.org/10.1016/S0013-7952\(99\)00090-3](https://doi.org/10.1016/S0013-7952(99)00090-3)
- Gupta, A. S., Seshagiri Rao, K. (1998). Index properties of weathered rocks: inter-relationships and applicability. *Bulletin of Engineering Geology and the Environment*, 57, 161-172.
- Gupta, D., Natarajan, N. (2021). Prediction of uniaxial compressive strength of rock samples using density weighted least squares twin support vector regression. *Neural Computing and Applications*, 33, 15843-15850. <https://doi.org/10.1007/s00521-021-06204-2>
- Hashemi, M., Moghaddas, S., Ajalloeian, R. (2010). Application of rock mass characterization for determining the mechanical properties of rock mass: a comparative study. *Rock Mechanics and Rock Engineering*, 43, 305-320. <https://doi.org/10.1007/s00603-009-0048-y>
- Han, D., Zhu, J., Leung, Y. F. (2022). Failure strength and fracture characteristics of rock with discontinuity under indirect tension. *Journal of Rock Mechanics and Geotechnical Engineering*, 14(6), 1810-1822. <https://doi.org/10.1016/j.jrmge.2022.02.007>
- Han, G., Jing, H., Jiang, Y., Liu, R., Su, H., Wu, J. (2018). The effect of joint dip angle on the mechanical behavior of infilled jointed rock masses under uniaxial and biaxial compressions. *Processes*, 6(5), 49. <https://doi.org/10.3390/pr6050049>
- Hoek, E. (1977). Rock mechanics laboratory testing in the context of a consulting engineering organization. *International Journal of Rock Mechanics and Mining Sciences & Geomechanics Abstracts*, 14(2), 93-101. [https://doi.org/10.1016/0148-9062\(77\)90201-7](https://doi.org/10.1016/0148-9062(77)90201-7)
- Hoek, E. (1983). Strength of jointed rock masses. *Geotechnique*, 33(3), 187-223. <https://doi.org/10.1680/geot.1983.33.3.187>
- Hoek, E. (2000). *Practical Rock Engineering*. Internet reference: www.rocksience.com, Rocsience.

- Hoek, E., Brown, E. T. (1997). Practical estimates of rock mass strength. *International journal of rock mechanics and mining sciences*, 34(8), 1165-1186. [https://doi.org/10.1016/S1365-1609\(97\)80069-X](https://doi.org/10.1016/S1365-1609(97)80069-X)
- Hoek, E., Carranza-Torres, C., Corkum, B. (2002). Hoek-Brown failure criterion-2002 edition. *Proceedings of NARMS-Tac*, 1(1), 267-273
- Huang, F., Shen, J., Cai, M., Xu, C. (2019). An empirical UCS model for anisotropic blocky rock masses. *Rock Mechanics and Rock Engineering*, 52, 3119-3131. <https://doi.org/10.1007/s00603-019-01771-2>
- Hudson, J. A., Harrison, J. P. (2000). *Engineering rock mechanics: an introduction to the principles*. Elsevier.
- ISRM. (1978). Suggested methods for the quantitative description of discontinuities in rock masses. *International Society for Rock Mechanics, Commission on Standardization of Laboratory and Field Tests. International Journal of Rock Mechanics and Mining Science & Geomechanics Abstracts*, 15, 319-368. [https://doi.org/10.1016/0148-9062\(78\)91472-9](https://doi.org/10.1016/0148-9062(78)91472-9)
- Itasca, UDEC. (2004). *Universal distinct element code*. Itasca Consulting Group, Minneapolis, Minn.
- Jaberi, A., Zare, S. (2025). Numerical Evaluation of the Influence of Fracture Geometry Parameter on Deformability, Strength, and Poisson's Ratio of 3d-Fractured Rock. *Indian Geotechnical Journal*, 1-20. <https://doi.org/10.1007/s40098-025-01163-0>
- Jade, S., Sitharam, T. G. (2003). Characterization of strength and deformation of jointed rock mass based on statistical analysis. *International journal of Geomechanics*, 3(1), 43-54. [https://doi.org/10.1061/\(ASCE\)1532-3641\(2003\)3:1\(43\)](https://doi.org/10.1061/(ASCE)1532-3641(2003)3:1(43))
- Jahed Armaghani, D., Safari, V., Fahimifar, A., Mohd Amin, M. F., Monjezi, M., Mohammadi, M. A. (2018). Uniaxial compressive strength prediction through a new technique based on gene expression programming. *Neural Computing and Applications*, 30, 3523-3532. <https://doi.org/10.1007/s00521-017-2939-2>
- Ji, S., Wang, Q., Marcotte, D., Salisbury, M. H., Xu, Z. (2007). P wave velocities, anisotropy and hysteresis in ultrahigh-pressure metamorphic rocks as a function of confining pressure. *Journal of Geophysical Research: Solid Earth*, 112(B9). <https://doi.org/10.1029/2006JB004867>
- Jia, C., Chen, F., Zhou, S., Lei, M., Huang, J., Zheng, Y. (2025). Effect of joint density on mechanical behavior of rock mass: Insight from 3D printing tests and DEM simulation. *Engineering Fracture Mechanics*, 315, 110846. <https://doi.org/10.1016/j.engfracmech.2025.110846>
- Jing, H., Nikafshan Rad, H., Hasanipanah, M., Jahed Armaghani, D., Qasem, S. N. (2021). Design and implementation of a new tuned hybrid intelligent model to predict the uniaxial compressive strength of the rock using SFS-ANFIS. *Engineering with Computers* 37, 2717-2734. <https://doi.org/10.1007/s00366-020-00977-1>
- Jing, L., Hudson, J. A. (2002). Numerical methods in rock mechanics. *International Journal of Rock Mechanics and Mining Sciences*, 39(4), 409-427. [https://doi.org/10.1016/S1365-1609\(02\)00065-5](https://doi.org/10.1016/S1365-1609(02)00065-5)
- Jing, L., Stephansson, O. (2007). *Fundamentals of discrete element methods for rock engineering: theory and applications*. Elsevier.
- Kahraman, S., Yeken, T. (2008). Determination of physical properties of carbonate rocks from P-wave velocity. *Bulletin of Engineering Geology and the Environment*, 67, 277-281. <https://doi.org/10.1007/s10064-008-0139-0>
- Karakul, H., Ulusay, R. (2013). Empirical correlations for predicting strength properties of rocks from P-wave velocity under different degrees of saturation. *Rock mechanics and rock engineering*, 46, 981-999. <https://doi.org/10.1007/s00603-012-0353-8>
- Kayabali, K., Selcuk, L. (2010). Nail penetration test for determining the uniaxial compressive strength of rock. *International Journal of Rock Mechanics and Mining Sciences*, 47(2), 265-271. <https://doi.org/10.1016/j.ijrmms.2009.09.010>
- Kim, B. H., Cai, M., Kaiser, P. K., Yang, H. S. (2007). Estimation of block sizes for rock masses with non-persistent joints. *Rock mechanics and rock engineering*, 40(2), 169. <https://doi.org/10.1007/s00603-006-0093-8>
- Kulatilake, P. H. S. W. (1985). Fitting Fisher distributions to discontinuity orientation data. *Journal of Geological Education*, 33(5), 266-269. <https://doi.org/10.1016/0022-1368-33.5.266>
- Kulatilake, P. H. S. W., Wu, T. H. (1984). Estimation of mean trace length of discontinuities. *Rock Mechanics and Rock Engineering*, 17(4), 215-232. <https://doi.org/10.1007/BF01032335>
- Kulatilake, P. H. S. W., Liang, J., Gao, H. (2001). Experimental and numerical simulations of jointed rock block strength under uniaxial loading. *Journal of Engineering Mechanics*, 127(12), 1240-1247. [https://doi.org/10.1061/\(ASCE\)0733-9399\(2001\)127:12\(1240\)](https://doi.org/10.1061/(ASCE)0733-9399(2001)127:12(1240))
- Kulatilake, P. H., Shu, B. (2015). Prediction of rock mass deformations in three dimensions for a part of an open pit mine and comparison with field deformation monitoring data. *Geotechnical and Geological Engineering*, 33, 1551-1568.
- Kumar, S., Halder, P., Manna, B., Sharma, K. G. (2018). Influence of Joint Orientation on the Behavior of Dam Resting on Jointed Rock Mass Under Static Condition. *Indian Geotechnical Journal*, 48, 650-662.
- Kumar, S., Tiwari, G., Parameswaran, V., Das, A. (2022). Rate-dependent mechanical behavior of jointed rock with an impersistent joint under different infill conditions. *Journal of Rock Mechanics and Geotechnical Engineering*, 14(5), 1380-1393. <https://doi.org/10.1016/j.jrmge.2022.05.002>
- Lama, R.D., Vutukuri, V. S. (1978). *Handbook on mechanical properties of rocks-testing techniques and results-volume iii*, 3(2).
- Lawal, A. I., Kwon, S., Aladejare, A. E., Oniyide, G. O. (2022). Prediction of the static and dynamic mechanical properties of sedimentary rock using soft computing methods. *Geomechanics and Engineering*, 28(3), 313. <https://doi.org/10.12989/gae.2022.28.3.313>
- Lawankar, S. M., Tiwari, G., Pandit, B. (2024). Numerical simulation of flaw inclination effects on rock-like specimen behavior using UDEC. In *New Challenges in Rock Mechanics and Rock Engineering*, CRC Press, 1277-1282.
- Lei, Y., Zhou, S., Luo, X., Niu, S., Jiang, N. (2022). A comparative study of six hybrid prediction models for uniaxial compressive strength of rock based on swarm intelligence optimization algorithms. *Frontiers in Earth Science*, 10, 930130. <https://doi.org/10.3389/feart.2022.930130>
- Li, C., Zhou, J., Dias, D., Du, K., Khandelwal, M. (2023). Comparative evaluation of empirical approaches and artificial intelligence techniques for predicting uniaxial compressive strength of rock. *Geosciences*, 13(10), 294. <https://doi.org/10.3390/geosciences13100294>
- Li, H., Zhao, X., Wang, Y., Dai, B., Zhu, Q., Chang, J. (2025). Research on the Estimation of Rock Mass Compressive Strength Based on Critical Strain Theory. *Mining, Metallurgy & Exploration*, 1-12. <https://doi.org/10.1007/s42461-025-01178-4>
- Li, Y., Zeng, J., Suhatrio, M., Marzouki, R., Denic, N., Almuaythir, S., Hussein M. M. A., Toghroli, E. (2023). Analyzing the shear strength of jointed magmatic rock mass excavatability using the hybridization of metaheuristic model of ELM-SVM. *Acta Geotechnica*, 18(4), 1793-1819. <https://doi.org/10.1007/s11440-022-01596-4>
- Li, Y. M., Zhao, G. F. (2021). A numerical integrated approach for the estimation of the uniaxial compression strength of rock from point load tests. *International Journal of Rock Mechanics and Mining Sciences*, 148, 104939. <https://doi.org/10.1016/j.ijrmms.2021.104939>
- Meulenkamp, F., Grima, M. A. (1999). Application of neural networks for the prediction of the unconfined compressive strength (UCS) from Equotip hardness. *International Journal of rock mechanics and mining sciences*, 36(1), 29-39. [https://doi.org/10.1016/S0148-9062\(98\)00173-9](https://doi.org/10.1016/S0148-9062(98)00173-9)
- Min, K. B., Jing, L. (2003). Numerical determination of the equivalent elastic compliance tensor for fractured rock masses using the distinct element method. *International Journal of Rock Mechanics and Mining Sciences*, 40(6), 795-816. [https://doi.org/10.1016/S1365-1609\(03\)00038-8](https://doi.org/10.1016/S1365-1609(03)00038-8)
- Mishra, D. A., Basu, A. (2013). Estimation of uniaxial compressive strength of rock materials by index tests using regression analysis and fuzzy inference system. *Engineering Geology*, 160, 54-68. <https://doi.org/10.1016/j.enggeo.2013.04.004>
- Mokhtarian, H., Moomivand, H., Moomivand, H. (2020). Effect of infill material of discontinuities on the failure criterion of rock under triaxial compressive stresses. *Theoretical and Applied Fracture Mechanics*, 108, 102652. <https://doi.org/10.1016/j.tafmec.2020.102652>

- Noorian-Bidgoli, M. (2014). Strength and deformability of fractured rocks. Doctoral dissertation, KTH Royal Institute of Technology.
- Noorian-Bidgoli, M., Jing, L. (2014). Anisotropy of strength and deformability of fractured rocks. *Journal of Rock Mechanics and Geotechnical Engineering*, 6(2), 156-164. <https://doi.org/10.1016/j.jrmge.2014.01.009>
- Noorian-Bidgoli, M., Zhao, Z., Jing, L. (2013). Numerical evaluation of strength and deformability of fractured rocks. *Journal of Rock Mechanics and Geotechnical Engineering*, 5(6), 419-430. <https://doi.org/10.1016/j.jrmge.2013.09.002>
- Özsan, A., Akın, M. (2002). Engineering geological assessment of the proposed Uruş dam, Turkey. *Engineering geology*, 66(3-4), 271-281. [https://doi.org/10.1016/S0013-7952\(02\)00047-9](https://doi.org/10.1016/S0013-7952(02)00047-9)
- Palmström, A. (1996). Characterizing rock masses by the RMI for use in practical rock engineering: Part 1: The development of the Rock Mass index (RMI). *Tunnelling and underground space technology*, 11(2), 175-188. [https://doi.org/10.1016/0886-7798\(96\)00015-6](https://doi.org/10.1016/0886-7798(96)00015-6)
- Pine, R.J., Harrison, J.P. (2003). Rock mass properties for engineering design. *Quarterly journal of engineering geology and hydrogeology*, 36(1), 5-16. <https://doi.org/10.1144/1470-923601-031>
- Plinninger, R., Käsling, H., Thuro, K., Spaun, G. (2003). Testing conditions and geomechanical properties influencing the CERCHAR abrasiveness index (CAI) value. *International journal of rock mechanics and mining sciences*, 40(2), 259-263. [https://doi.org/10.1016/S1365-1609\(02\)00140-5](https://doi.org/10.1016/S1365-1609(02)00140-5)
- Priest, S.D. (1993). *Discontinuity analysis for rock engineering*. Springer Science & Business Media.
- Priest, S. D., Hudson, J. A. (1976). Discontinuity spacings in rock. *International Journal of Rock Mechanics and Mining Sciences & Geomechanics Abstracts*, 13(5), 135-148. [https://doi.org/10.1016/0148-9062\(76\)90818-4](https://doi.org/10.1016/0148-9062(76)90818-4)
- Qi, S., Macciotta, R., Shou, K. J., Saroglou, C. (2020). Preface to the Special Issue on: Advances in rock mass engineering geomechanics. *Engineering Geology*, 272, 105642. <https://doi.org/10.1016/j.enggeo.2020.105642>
- Que, X., Zhu, Z., He, Y., Niu, Z., Huang, H. (2023). Strength and deformation characteristics of irregular columnar jointed rock mass: A combined experimental and theoretical study. *Journal of Rock Mechanics and Geotechnical Engineering*, 15(2), 429-441. <https://doi.org/10.1016/j.jrmge.2022.03.007>
- Que, X., Zhu, Z., Niu, Z., Lu, W. (2021). Estimating the strength and deformation of columnar jointed rock mass based on physical model test. *Bulletin of Engineering Geology and the Environment*, 80, 1557-1570. <https://doi.org/10.1007/s10064-020-01974-w>
- Rahmouni, A., Boulanouar, A., Boukalouch, M., Samaouli, A., Harnafi, M., Sebbani, J. (2013). Prediction of porosity and density of calcarenite rocks from P-wave velocity measurements. *International Journal of Geosciences*, 4, 1292-1299.
- Ramna, Y. V., Venkatanarayana, B. (1973). Laboratory studies on Kolar rocks. *International Journal of Rock Mechanics and Mining Sciences & Geomechanics Abstracts*, 10(5), 465-489. [https://doi.org/10.1016/0148-9062\(73\)90028-4](https://doi.org/10.1016/0148-9062(73)90028-4)
- Reik, G., Zacas, M. (1978). Strength and deformation characteristics of jointed media in true triaxial compression. *International Journal of Rock Mechanics and Mining Sciences & Geomechanics Abstracts*, 15(6), 295-303. [https://doi.org/10.1016/0148-9062\(78\)91470-5](https://doi.org/10.1016/0148-9062(78)91470-5)
- Rives, T., Razack, M., Petit, J.P., Rawnsley, K.D. (1992). Joint spacing: analogue and numerical simulations. *Journal of structural geology*, 14(8-9), 925-937. [https://doi.org/10.1016/0191-8141\(92\)90024-Q](https://doi.org/10.1016/0191-8141(92)90024-Q)
- Rix, G. J., Wainaina, N., Ebrahimi, A., Bachus, R. C., Limas, M., Sancio, R., Fait, B., Mayne, P. W. (2019). *Manual on subsurface investigations*. Washington, DC: The National Academies Press. <https://doi.org/10.17226/25379>
- Seshagiri Rao, K. (2020). Characterization, modelling and engineering of rocks and rockmasses. *Indian Geotechnical Journal*, 50, 1-95.
- Shan, R., Liu, N., Sun, P., Zhao, Z., Dong, R., Dou, H., Meng, H., Bai, Y. (2025). Experimental and numerical simulation study of rough jointed rock samples under triaxial compression conditions. *Engineering Fracture Mechanics*, 314, 110707. <https://doi.org/10.1016/j.engfracmech.2024.110707>
- Shimizu, H., Koyama, T., Ishida, T., Chijimatsu, M., Fujita, T., Nakama, S. (2010). Distinct element analysis for Class II behavior of rocks under uniaxial compression. *International Journal of Rock Mechanics and Mining Sciences*, 47(2), 323-333. <https://doi.org/10.1016/j.ijrmms.2009.09.012>
- Singh, B., Goel, R. K. (2011). *Engineering rock mass classification*. Boston: Butterworth-Heinemann.
- Singh, M., Khalkho, P. (2023). Prediction of Strength and Modulus of Jointed Rocks Using P-wave Velocity. *Geotechnical and Geological Engineering*, 1-22. <https://doi.org/10.1007/s10706-023-02478-6>
- Song, J. J. (2006). Estimation of areal frequency and mean trace length of discontinuities observed in non-planar surfaces. *Rock mechanics and rock engineering*, 39, 131-146. <https://doi.org/10.1007/s00603-005-0060-9>
- Sonmez, H., Ulusay, R. (1999). Modifications to the geological strength index (GSI) and their applicability to stability of slopes. *International Journal of Rock Mechanics and Mining Sciences*, 36(6), 743-760. [https://doi.org/10.1016/S0148-9062\(99\)00043-1](https://doi.org/10.1016/S0148-9062(99)00043-1)
- Starzec, P. (1999). Dynamic elastic properties of crystalline rocks from south-west Sweden. *International Journal of Rock Mechanics and Mining Sciences*, 36(2), 265-272. [https://doi.org/10.1016/S0148-9062\(99\)00011-X](https://doi.org/10.1016/S0148-9062(99)00011-X)
- Szlavin, J. (1974). Relationships between some physical properties of rock determined by laboratory tests. *International Journal of Rock Mechanics and Mining Sciences & Geomechanics Abstracts*, 11(2), 57-66. [https://doi.org/10.1016/0148-9062\(74\)92649-7](https://doi.org/10.1016/0148-9062(74)92649-7)
- Tang, C. A., Liu, H., Lee, P. K. K., Tsui, Y., Tham, L. (2000). Numerical studies of the influence of microstructure on rock failure in uniaxial compression-part I: effect of heterogeneity. *International Journal of Rock Mechanics and Mining Sciences*, 37(4), 555-569. [https://doi.org/10.1016/S1365-1609\(99\)00121-5](https://doi.org/10.1016/S1365-1609(99)00121-5)
- Tang, J. Z., Yang, S. Q., Zhao, Y. L., Tian, W. L. (2020). Experimental and numerical modeling of the shear behavior of filled rough joints. *Computers and Geotechnics*, 121, 103479. <https://doi.org/10.1016/j.compgeo.2020.103479>
- Tiryaki, B. (2008). Predicting intact rock strength for mechanical excavation using multivariate statistics, artificial neural networks, and regression trees. *Engineering Geology*, 99(1-2), 51-60. <https://doi.org/10.1016/j.enggeo.2008.02.003>
- Ulusay, R., Hudson, J. A. (2007). *The complete ISRM suggested methods for rock characterization, testing and monitoring: 1974-2006*. ISRM Turkish National Group, Ankara, Turkey.
- Wang, Y., Aladejare, A. E. (2015). Selection of site-specific regression model for characterization of uniaxial compressive strength of rock. *International Journal of Rock Mechanics and Mining Sciences*, 75, 73-81. <https://doi.org/10.1016/j.ijrmms.2015.01.008>
- Wang, Y., Yang, H., Song, K., Chen, C., Li, H., Li, X. (2025). The influence of joint distribution characteristics on the mechanical properties, fracture mechanisms, and energy characteristics of rock masses under stress conditions. *Computers and Geotechnics*, 178, 106933. <https://doi.org/10.1016/j.compgeo.2024.106933>
- Wang, Z., Wang, M., Zhou, L., Zhu, Z., Shu, Y., Peng, T. (2022). Research on uniaxial compression strength and failure properties of stratified rock mass. *Theoretical and Applied Fracture Mechanics*, 121, 103499. <https://doi.org/10.1016/j.tafmec.2022.103499>
- Wines, D. R., Lilly, P. A., 2003. Estimates of rock joint shear strength in part of the Fimiston open pit operation in Western Australia. *International Journal of Rock Mechanics and Mining Sciences*, 40(6), 929-937. [https://doi.org/10.1016/S1365-1609\(03\)00020-0](https://doi.org/10.1016/S1365-1609(03)00020-0)
- Wu, Y., Zhao, Y., Tang, P., Wang, W., Jiang, L. (2022). Analysis of the mechanical properties and failure modes of rock masses with nonpersistent joint networks. *Geomechanics and Engineering*, 30(3), 281. <https://doi.org/10.12989/gae.2022.30.3.281>

- Xu, H., Zhang, Z., Zhang, Y. J., Jiang, Q., Qiu, S. L., Zhou, Y. Y., Feng, G. L. (2024). Effects of natural stiff discontinuities on the deformation and failure mechanisms of deep hard rock under true triaxial conditions. *Engineering Failure Analysis*, 158, 108034. <https://doi.org/10.1016/j.engfailanal.2024.108034>
- Xu, T., Ranjith, P. G., Wasantha, P. L. P., Zhao, J., Tang, C. A., Zhu, W. C. (2013). Influence of the geometry of partially-spanning joints on mechanical properties of rock in uniaxial compression. *Engineering Geology*, 167, 134-147. <https://doi.org/10.1016/j.enggeo.2013.10.011>
- Yaşar, E., Erdoğan, Y. (2004). Estimation of rock physicochemical properties using hardness methods. *Engineering Geology*, 71(3-4), 281-288. [https://doi.org/10.1016/S0013-7952\(03\)00141-8](https://doi.org/10.1016/S0013-7952(03)00141-8)
- Yu, Z., Zhou, J., Hu, L. (2023). Prediction of compressive strength of granite: use of machine learning techniques and intelligent system. *Earth Science Informatics*, 16(4), 4113-4129. <https://doi.org/10.1007/s12145-023-01145-x>
- Zhang, H., Wu, S., Zhang, Z. (2022). Prediction of uniaxial compressive strength of rock via genetic algorithm-selective ensemble learning. *Natural Resources Research*, 31(3), 1721-1737. <https://doi.org/10.1007/s11053-022-10065-4>
- Zhang, L. (2010). Estimating the strength of jointed rock masses. *Rock Mechanics and Rock Engineering*, 43, 391-402. <https://doi.org/10.1007/s00603-009-0065-x>
- Zhang, L. (2016). *Engineering properties of rocks*. Butterworth-Heinemann.
- Zhang, Z., Zhang, Q., Ma, K., Deng, J. (2025). Study on the Effects of Microstructural Heterogeneity on the Mechanical Behavior and Failure Process of Brittle Rocks Based on DEM. *Rock Mechanics and Rock Engineering*, 1-22. <https://doi.org/10.1007/s00603-024-04322-6>
- Zhao, J., Tong, H., Yuan, J., Wang, Y., Cui, J., Shan, Y. (2025). Three-dimensional strength and deformation characteristics of calcareous sand under various stress paths. *Bulletin of Engineering Geology and the Environment*, 84(1), 61. <https://doi.org/10.1007/s10064-025-04083-8>
- Zhao, Y., Zhang, L., Wang, W., Liu, Q., Tang, L., Cheng, G. (2020). Experimental study on shear behavior and a revised shear strength model for infilled rock joints. *International Journal of Geomechanics*, 20(9), p.04020141. [https://doi.org/10.1061/\(ASCE\)GM.1943-5622.0001781](https://doi.org/10.1061/(ASCE)GM.1943-5622.0001781)
- Zhong, Z., Deng, R., Zhang, J., Hu, X. (2020). Fracture properties of jointed rock infilled with mortar under uniaxial compression. *Engineering Fracture Mechanics*, 228, 106822. <https://doi.org/10.1016/j.engfracmech.2019.106822>
- Zorlu, K., Gokceoglu, C., Ocakoglu, F., Nefeslioglu, H. A., Acikalin, S. J. E. G. (2008). Prediction of uniaxial compressive strength of sandstones using petrography-based models. *Engineering Geology*, 96(3-4), 141-158. <https://doi.org/10.1016/j.enggeo.2007.10.009>